

Control of Double-Inverted Pendulum

Group F: Pruthak Joshi, Aruul Mozhi Varman Senthilkumar, Shubham Wani

Final Project

MAE277: Advanced Digital Control for Mechatronic Systems

Prof. Tsu-Chin Tsao

Winter 2023

Contents

1 Objective	3
1.1 Approach	3
1.2 Dynamics of the motor	3
1.3 Dynamics of the double pendulum	4
1.4 System Identification	4
1.5 Simulation	4
1.6 Hardware	5
1.7 Controller	6
2 Controller Analysis	8
2.1 Sensitivity and Complementary Sensitivity	8
3 Hardware Implementation	11
3.1 Swinging - Up and Down	11
3.2 Integral	11
3.3 Integral + Oscillator	12
3.4 Repetitive + Feedforward	13
4 Disturbance Rejection	14
4.1 Integral	15
4.2 Integral + Oscillator	16
4.3 Repetitive + Feedforward Control	17
5 Error Analysis	18
5.1 Integral	18
5.2 Integral + Oscillator	18
5.3 Repetitive + Feedback	18
6 Conclusions	19

1 Objective

To swing the double-pendulum from initially vertically down position to the vertically up position at t=1 second and subject to 1 step disturbance of 0.01 Nm at t=5 second by digital control with as large sampling time as possible.

1.1 Approach

The motor-driver setup was placed opposite to another motor-driver setup. Motor 1 was uncontrolled and observed whereas motor 2 was controlled but unobserved. The encoder readings for both were read by the same TI C2000 controller. The appropriate control voltage was applied to motor 2 and motor 1 had open circuit.



Figure 1: Hardware setup

1.2 Dynamics of the motor

The non-linear dynamics of an inverted pendulum are described as follows:

$$\begin{aligned} J_{pend} \frac{d\omega}{dt} &= b\omega + K_m i - mgl_c \sin\theta - T_d \\ L \frac{di}{dt} &= -Ri - K_m \omega + V_s u \\ J_{pend} &= J_{rotor} + ml_c^2 \end{aligned}$$

These are then linearized about the unstable equilibrium point. The three state model converts to a two state model as induction L and damping b is negligible for both the motors.

The reduced order state-space representation of the system is as follows:

$$\begin{aligned} x_1 &= \tilde{\theta}, x_2 = \tilde{\omega}, u = \tilde{i}, w = \tilde{T}_d \\ \begin{bmatrix} \frac{dx_1}{dt} \\ \frac{dx_2}{dt} \end{bmatrix} &= \begin{bmatrix} 0 & 1 \\ -\omega_n^2 & -2\zeta\omega_n \end{bmatrix} \begin{bmatrix} x_1 \\ x_2 \end{bmatrix} + \begin{bmatrix} 0 \\ K_u \end{bmatrix} u \begin{bmatrix} 0 \\ K_w \end{bmatrix} w \end{aligned} \quad (1)$$

where

$$\omega_n^2 = \frac{mgl_c \cos\theta_e}{J_{pend}}, 2\zeta\omega_n = \frac{K_m^2}{J_{pend}R}, K_u = \frac{K_m V_s}{J_{pend}R}, K_w = \frac{-1}{J_{pend}}$$

1.3 Dynamics of the double pendulum

The right inverted pendulum applies a force on the left pendulum via a torsional spring. Let k_c be the torsional spring constant. From equation 1, we know

$$\begin{aligned}\dot{x}_1 &= Ax_1 + Bu_1 - B_d T_{d_1} & y_1 &= Cx_1 \\ \dot{x}_2 &= Ax_2 + Bu_2 - B_d T_{d_2} & y_2 &= Cx_2 \\ u &= u_2 & y &= y_1 \\ T_{d_1} &= k_c(y_1 - y_2) + T_w & T_{d_2} &= k_c(y_2 - y_1)\end{aligned}$$

Representing the above in state space form, we get:

$$\begin{aligned}\begin{bmatrix} \dot{x}_1 \\ \dot{x}_2 \end{bmatrix} &= \begin{bmatrix} A - k_c B_d C & k_c B_d C \\ k_c B_d C & A - k_c B_d C \end{bmatrix} \begin{bmatrix} x_1 \\ x_2 \end{bmatrix} + \begin{bmatrix} 0 \\ B_d \end{bmatrix} u - \begin{bmatrix} B_d \\ 0 \end{bmatrix} T_w \\ y &= [C \quad 0] \begin{bmatrix} x_1 \\ x_2 \end{bmatrix}\end{aligned}\tag{2}$$

where A, B, C correspond to equation 1.

1.4 System Identification

The damping b and inductance L is negligible and assumed to be zero. The resistance for both motors is measured with a multimeter. The supply voltage V_s is measured at uniform increments of PWM duty cycle and fed into a 1D lookup table.

The torque constant and inertia of the motor are calculated using k and τ . The parameters are found by fitting a first-order model to the speed-time curve after a step input. A torsional spring applies an opposing torque proportional to the angular displacement from the neutral position. Hence, $\tau = k_c\theta$. To characterize k_c , we apply a known torque and measure the displacement. The slope of the graph is equal to k_c .

A stepped PWM signal was applied to the motor 2, which caused a stepped displacement in motor 2. Motor 1 was kept stationary using clamps. The torque applied is calculated using torque constant i.e. $\tau = k_t i$, where $i = V_s/R$.

The resistance was measured across the terminals to be $R = 8.985$ which evaluated the torque constant to be $K_t = 0.039 \text{Nm/A}$. The torque $\tau = K_t * V_{app}/R$ is calculated and plotted against the displacement. The torsional spring constant is $k_c = 0.095 \text{Nm/rad}$.

1.5 Simulation

The reduced order non-linear motor model was duplicated and a torsional force due to spring was added as a disturbance to each motor. A step input from 0 rad to πrad was applied to the system. The state observer feedback control (SOFC) with the integral term was used to estimate the state and track the reference. Estimator and controller gains were modified by changing the Q and R matrices to decrease estimator error and stabilize the inverted plant.

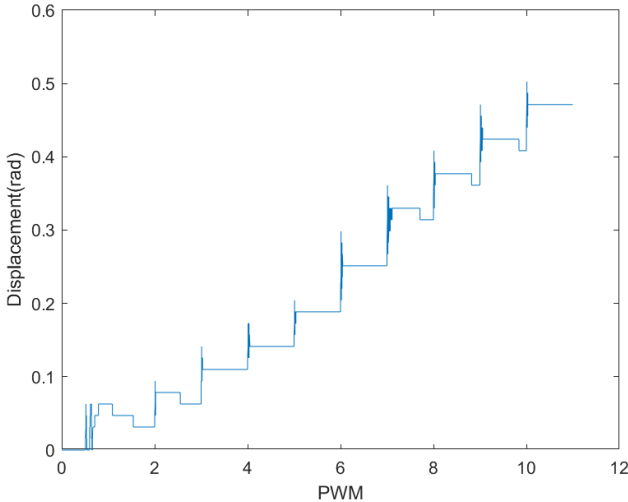


Figure 2: Displacement vs PWM percentage

PWM percent	Displacement(rad)
0	0
10	0.031
20	0.0628
30	0.110
40	0.141
50	0.188
60	0.251
70	0.314
80	0.361
90	0.408
100	0.471

Table 1: Torsional spring constant experiment data

1.6 Hardware

The quadrature motor encoder is read by the C2000 micro-controller and then read by the QEP block for both motors. The first encoder reading is used for the control but the second reading is not used. The motor 1 has open wiring and the motor 2 is controlled using a motor driver.

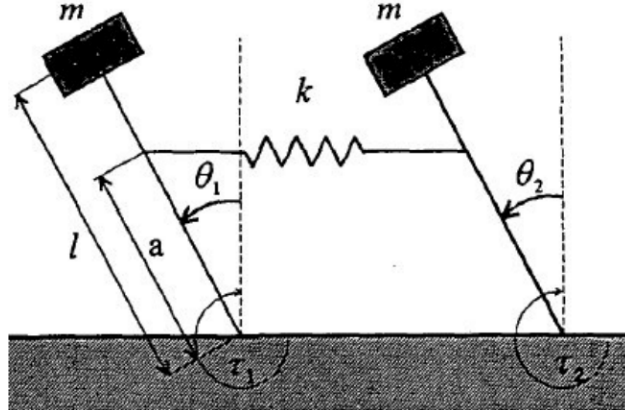


Figure 3: schematic of double pendulum

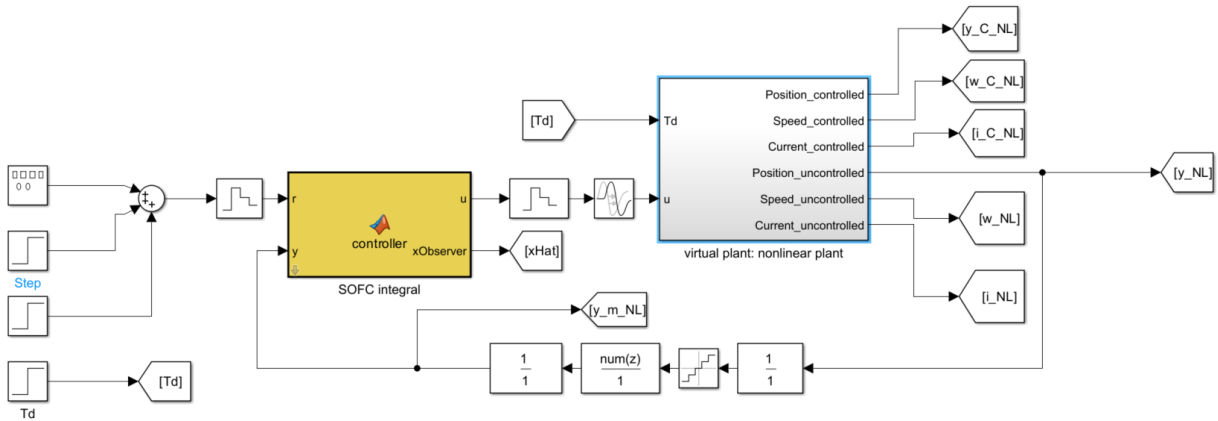


Figure 4: Simulink diagram

1.7 Controller

Controller synthesis:

SOFC+Integral controller was successful in stabilizing the inverted pendulum in both simulation and hardware.

$$AA = \begin{bmatrix} A_d - B_d * K_{sf} & B_d * K_{sf} \\ 0 & A_d - L_{pred} * C_d \end{bmatrix} BB = \begin{bmatrix} B_d * N & B_d & B_w \\ 0 & B_d & B_w \end{bmatrix} CC = \begin{bmatrix} C_d & 0 \\ -K_{sf} & -K_{sf} \\ -C_d & 0 \end{bmatrix} DD = \begin{bmatrix} 0 & 0 & 0 \\ N & 0 & 0 \\ 1 & 0 & 0 \end{bmatrix} \quad (3)$$

The L_{pred} gain and K_{sf} gains are calculated using LQR techniques.

The Q and R matrices for state estimator are as follows

$$Q_{pred} = \begin{bmatrix} 15 & 0 & 0 & 0 \\ 0 & 5000 & 0 & 0 \\ 0 & 0 & 0 & 0 \\ 0 & 0 & 0 & 0 \end{bmatrix} \quad R_{pred} = 1$$

The Q(2,2) term is set to a high value to reduce effects of process variation as angular velocity is a computed term and not directly measured. The Q(3,3) and Q(4,4) term are set to zero as they are estimated and not directly measured.

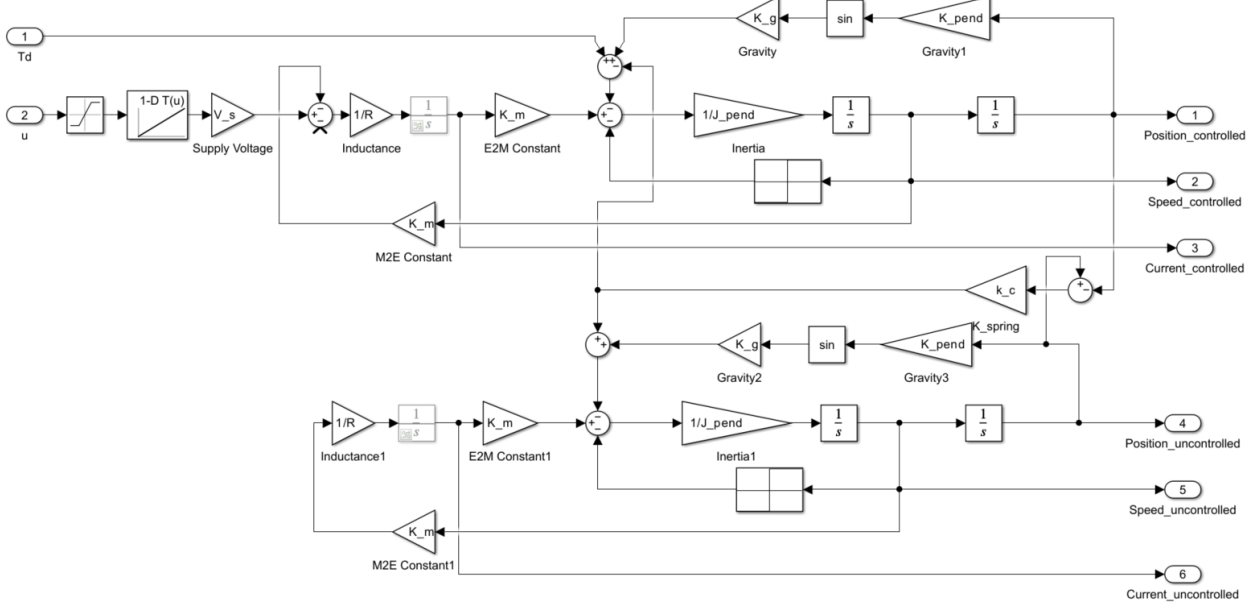


Figure 5: Figure

The Q and R matrices for controller are as follows

$$Q_{cont} = \begin{bmatrix} 0 & 0 & 0 & 0 & 0 \\ 0 & 0 & 0 & 0 & 0 \\ 0 & 0 & 1000 & 0 & 0 \\ 0 & 0 & 0 & 0 & 0 \\ 0 & 0 & 0 & 0 & 0.1 \end{bmatrix} \quad R_{cont} = 1$$

The Q(3,3) term corresponds to controlled position, so a high value is set. All other diagonal values are set to zero. The integral term is small but non-zero to help achieve steady state.

Integral+Oscillator with internal model was also successful in stabilizing the inverted pendulum in both simulation and hardware.

$$d_z = z^2 - (2 * \cos\omega_o T)z + 1, x_d(k+1) = A_d x_d(k) + B_d(y(k) - r(k)), u_d = -k_d x_d(k) \quad (4)$$

$$\begin{bmatrix} x_1(k+1) \\ x_2(k+1) \end{bmatrix} = \begin{bmatrix} 0 & 1 \\ -1 & 2\cos\omega_o T \end{bmatrix} \begin{bmatrix} x_1(k) \\ x_2(k) \end{bmatrix} + \begin{bmatrix} 0 \\ 1 \end{bmatrix} \cdot (y(k) - r(k)) \quad (5)$$

$$\begin{bmatrix} x_d(k+3) \\ x_d(k+2) \\ x_d(k+1) \end{bmatrix} = \begin{bmatrix} 2\cos\omega_o T s + 1 & -2\cos\omega_o T s - 1 & 1 \\ 1 & 0 & 0 \\ 0 & 1 & 0 \end{bmatrix} \begin{bmatrix} x_d(k+2) \\ x_d(k+1) \\ x_d(k) \end{bmatrix} + \begin{bmatrix} 1 \\ 0 \\ 0 \end{bmatrix} \cdot (y(k) - r(k)) \quad (6)$$

Oscillator states values are small (order of 10^{-6}) to preserve the nature of the matrix.

The closed loop poles for the system with the three controllers are as follows:

- Integral: $0.9961 \pm 0.0572i, 0.9788, 0.9884 \pm 0.0117i, 0.0098, 0.9894, 0.9968 \pm 0.039i$

- Integral + Oscillator: $0.9962 \pm 0.0572i$, 0.9794 , $0.9891 \pm 0.011i$, $0.9975 \pm 0.0059i$, 0.0098 , 0.9894 , $0.9968 \pm 0.039i$
- Repetitive + Feedback: $0.993 + 0.006i$, $0.993 - 0.006i$, 0.991 , 0.991 , 0.765 , 0.961 , 0.961

2 Controller Analysis

The performance and robustness of the designed controllers are analyzed using sensitivity and complementary functions. More formally, sensitivity is a measure of how much the output of a control system changes in response to changes in its inputs or disturbances. It is defined as the ratio of the change in output to the change in input or disturbance. A control system with high sensitivity will respond strongly to changes in input or disturbance, while a system with low sensitivity will be less responsive.

Complementary sensitivity, on the other hand, is a measure of how well a control system can reject disturbances that affect it. It is defined as the ratio of the change in output to the change in the disturbance. A control system with high complementary sensitivity will be able to reject disturbances effectively, while a system with low complementary sensitivity will be more susceptible to disturbances.

2.1 Sensitivity and Complementary Sensitivity

The sensitivity of LQG integral and LQG with integral and oscillator are presented in Fig. 9 & 10 respectively. In Fig. 10, there is a steep dip at 1hz this is an effect of the 1hz oscillator model in the closed-loop control. From the sensitivity functions, it can be seen that the controller with an oscillator has a poor disturbance rejection at low frequencies when compared to the integral control as the oscillator-based control has high sensitivity in this region. However, the oscillator-based internal model control is effective in countering the 1hz harmonic disturbance and this is clearly seen as a dip in sensitivity function at 1hz. While the controllers manage to track the reference, they are not robust to process variations and disturbances as seen in sensitivity functions.

The complimentary function for LQG with integral and LQR with oscillator are presented in Fig. 9 & 10. As expected it can be seen that the complementary sensitivity is close to unity at low frequencies and controller is good at low frequency disturbance rejection. In the case of LQG with oscillator, it can be seen that we have a very non-linear complementary sensitivity with high and low gains in most of the operating range and these traits are not very desirable for a robust controller.

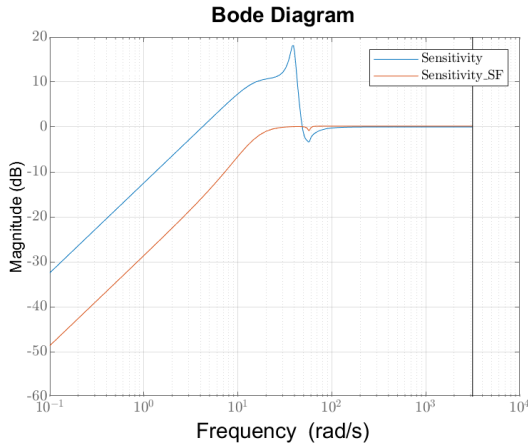


Figure 6: Sensitivity of LQG controller with integral action

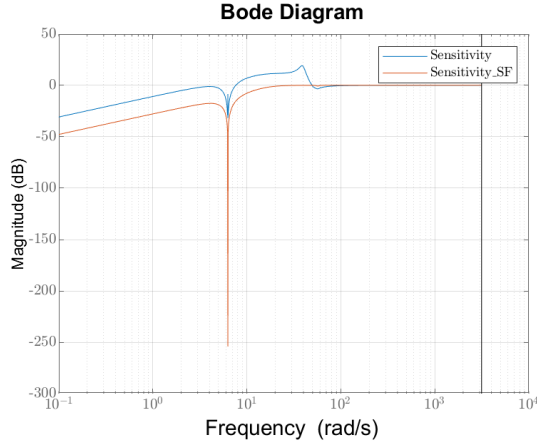


Figure 7: Sensitivity of LQG controller with integral action and 1hz oscillator

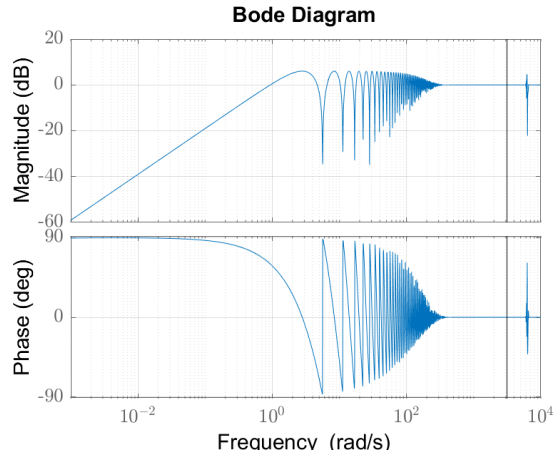


Figure 8: Sensitivity of Repetitive controller with feedforward action

Similarly, the sensitivity and complementary sensitivity functions for the repetitive controller are presented in Fig. 8 & 11. From Fig. 8, it can be seen that the sensitivity function of the repetitive control has steep dips. These dips improve the periodic disturbance rejection at these frequencies and is a direct effect of using the periodic disturbance model characterised by the Q-filter.

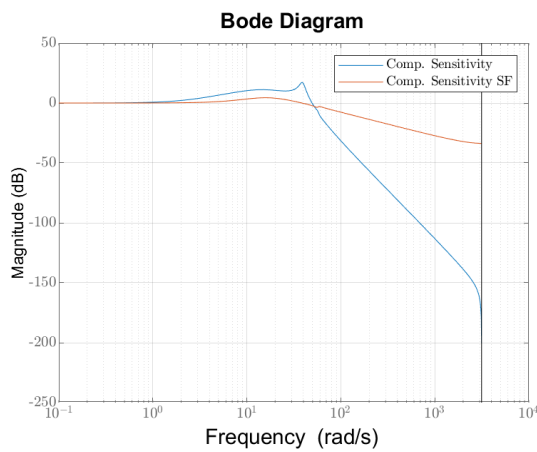


Figure 9: Complementary sensitivity of LQG with integral action

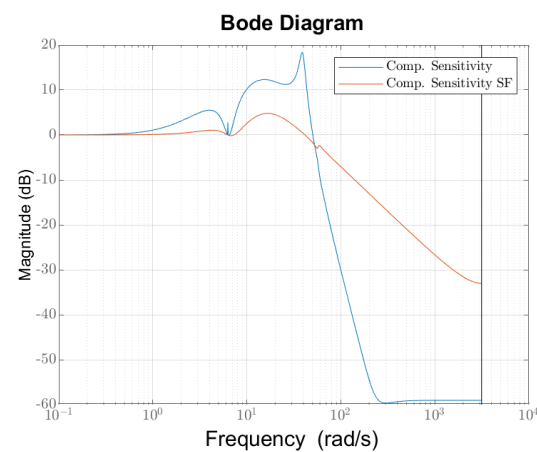


Figure 10: Complementary sensitivity of LQG with integral action and 1hz oscillator

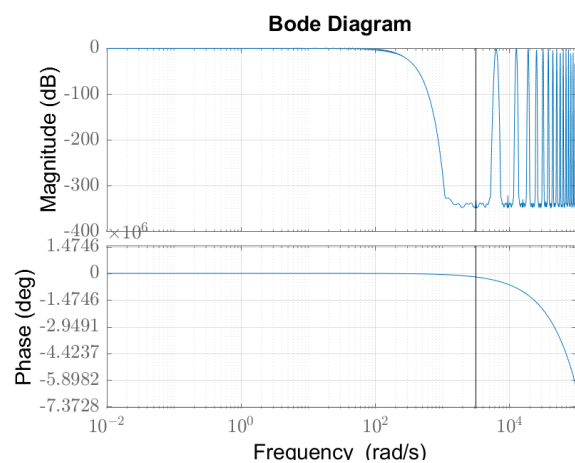


Figure 11: Complementary sensitivity of Repetitive controller with feedforward action

3 Hardware Implementation

3.1 Swinging - Up and Down

The system is linearized about the vertically upward position. Reference signal is given so that the system swings from the downward pendulum configuration to the upward pendulum configuration, and comes back to the downward pendulum position after some time. The simulation and hardware implementation results are shown in Figures 12a and 12b:

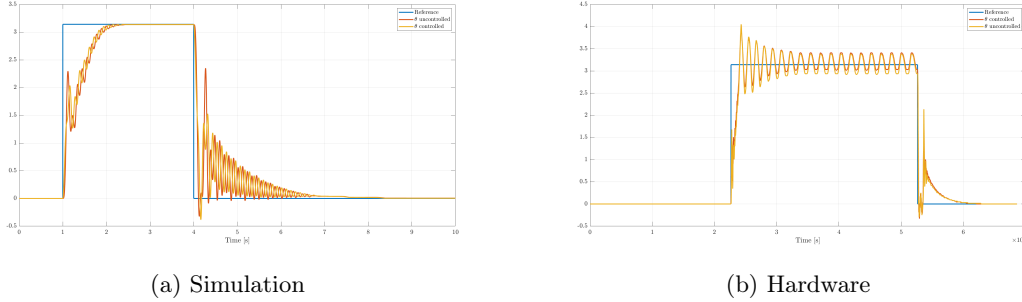


Figure 12: Simulation and Hardware implementation of the swinging up and down motion

We see that for the rising sequence, the hardware and simulation plots are slightly different. This might be due to a couple of reasons:

- Since the system is linearized about the vertically upward position, and the initial state is the vertically downward position, the system dynamics might not be correctly predicted.
- There could be room for improvement in the system identification.

However, we see that the behavior of the system in the downward step sequence is very similar to the behavior predicted by the simulations.

3.2 Integral

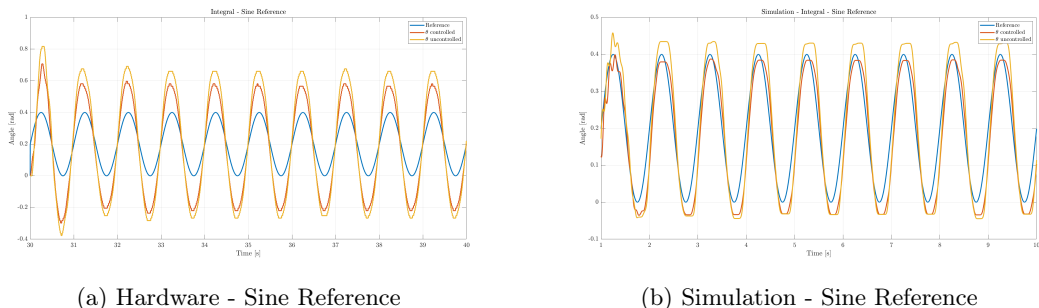
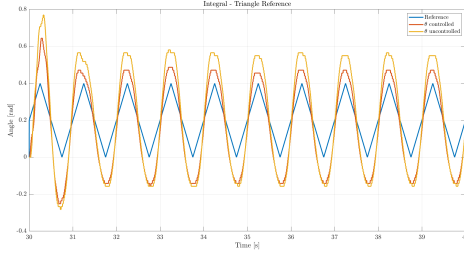
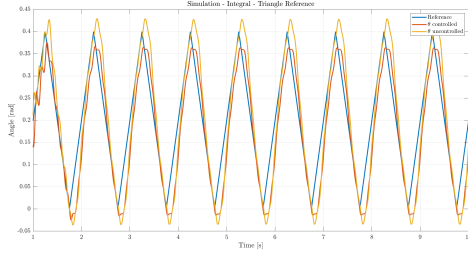


Figure 13: Hardware and Simulation comparison for Sine Reference Signal

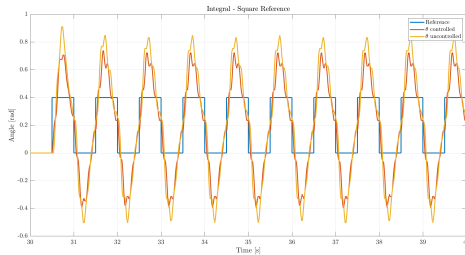


(a) Hardware - Triangle Reference

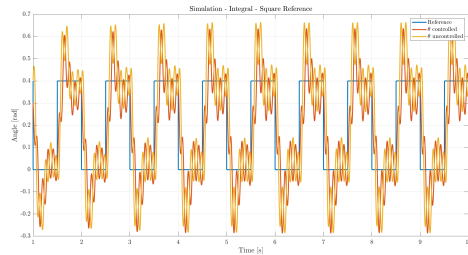


(b) Simulation - Triangle Reference

Figure 14: Hardware and Simulation comparison for Triangle Reference Signal



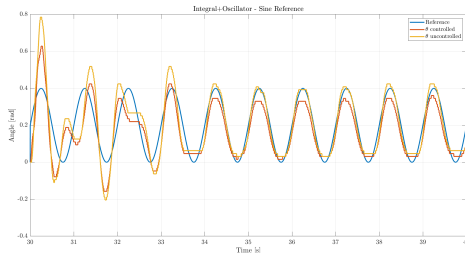
(a) Hardware - Square Reference



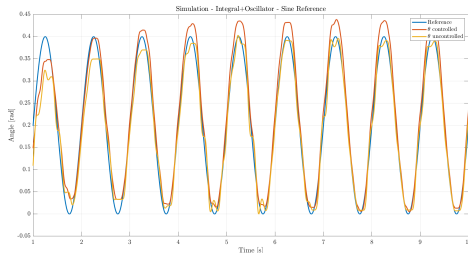
(b) Simulation - Square Reference

Figure 15: Hardware and Simulation comparison for Square Reference Signal

3.3 Integral + Oscillator

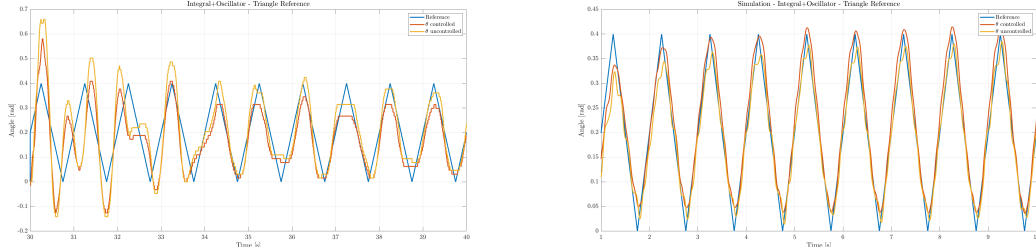


(a) Hardware - Sine Reference



(b) Simulation - Sine Reference

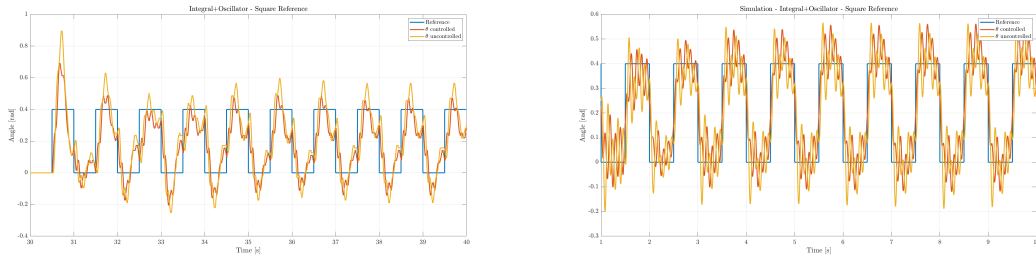
Figure 16: Hardware and Simulation comparison for Sine Reference Signal



(a) Hardware - Triangle Reference

(b) Simulation - Triangle Reference

Figure 17: Hardware and Simulation comparison for Triangle Reference Signal



(a) Hardware - Square Reference

(b) Simulation - Square Reference

Figure 18: Hardware and Simulation comparison for Square Reference Signal

3.4 Repetitive + Feedforward

Simulation was performed for the repetitive + feedforward controller. On trying to implement on the hardware, error was encountered due to the order of filter being 120, which was too high for the floating point precision of the microcontroller.

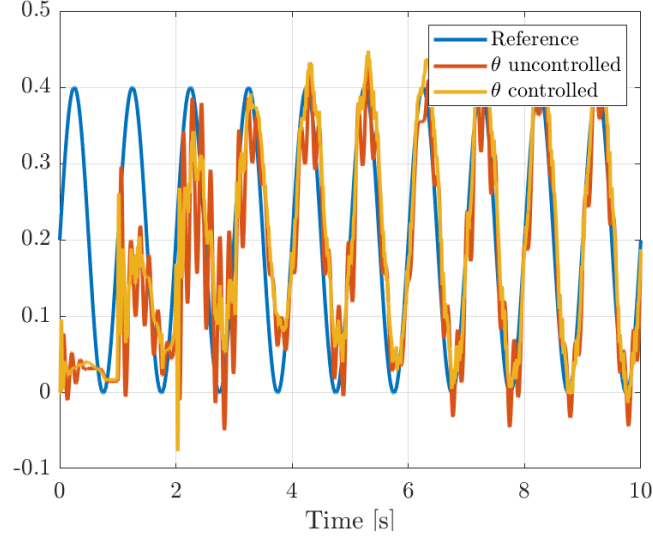


Figure 19: Simulation - Sine Reference

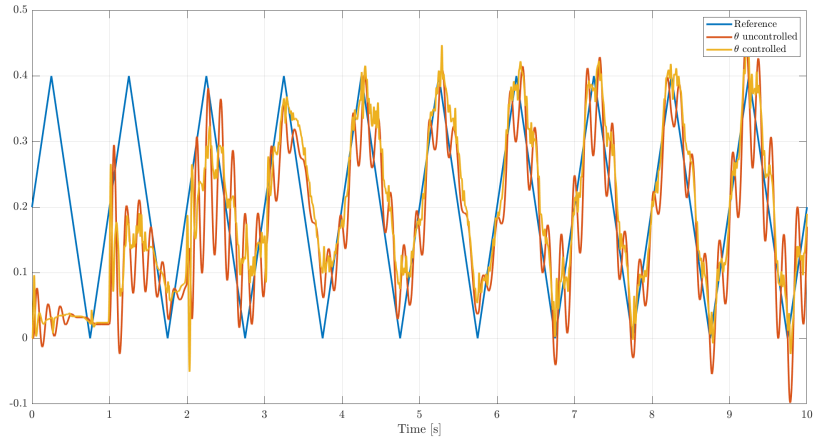


Figure 20: Simulation - Triangle Reference

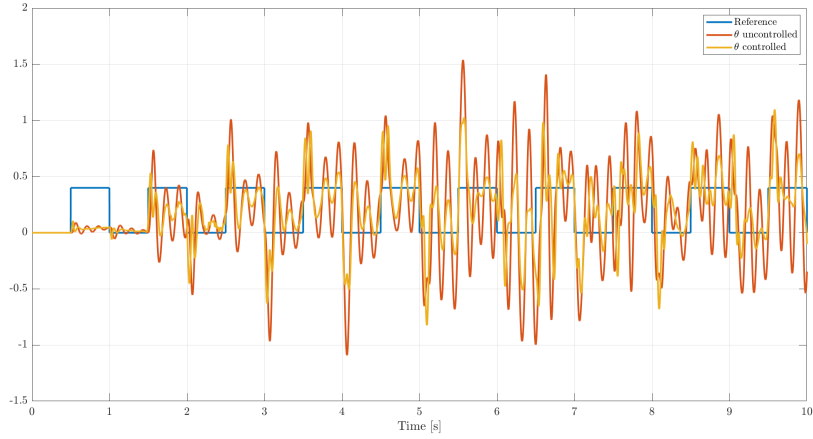


Figure 21: Simulation - Square Reference

4 Disturbance Rejection

A step disturbance of 0.01Nm was applied to the system at $t = 5 \text{ sec}$, and simulations were done to analyse the performance of the controllers. We observe that the integral and integral+oscillator controllers are able to reject the disturbance pretty well, however the repetitive+feedback controller needs more tuning for better disturbance rejection.

4.1 Integral

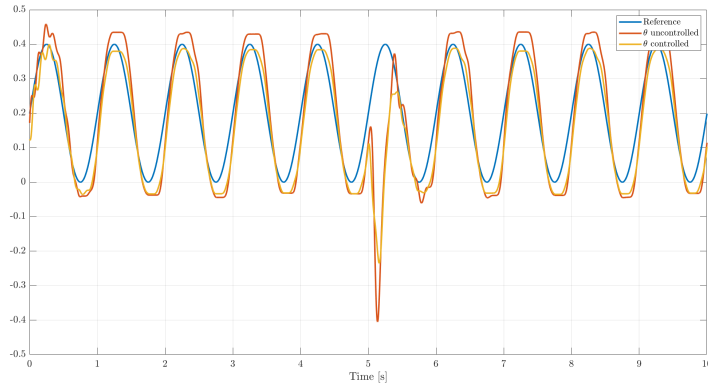


Figure 22: Disturbance Rejection for Sine Reference Signal

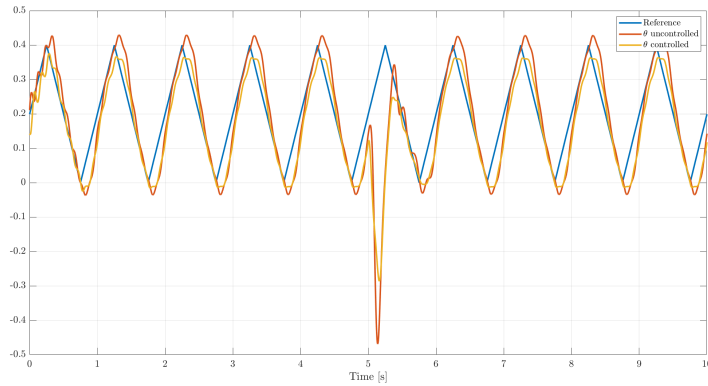


Figure 23: Disturbance Rejection for Triangle Reference Signal

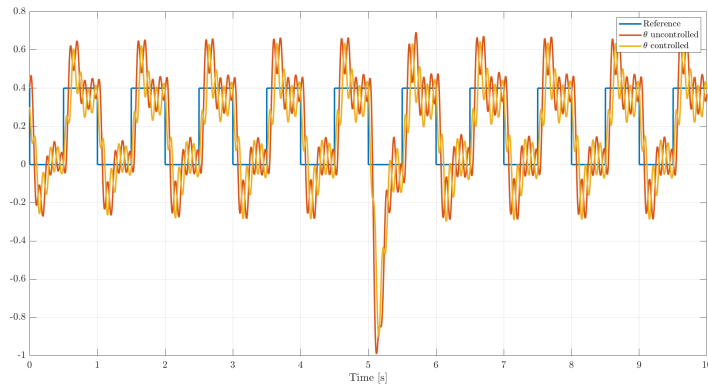


Figure 24: Disturbance Rejection for Square Reference Signal

4.2 Integral + Oscillator

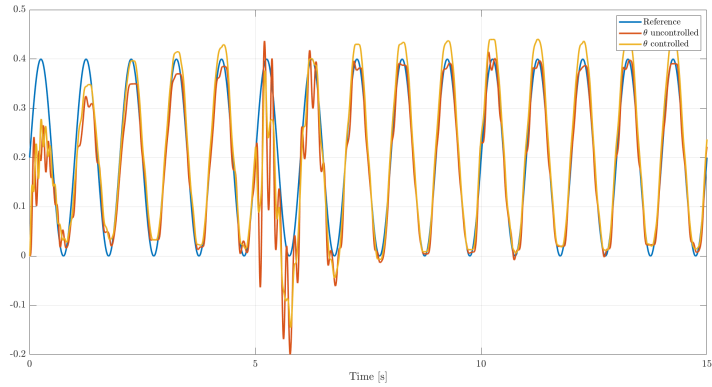


Figure 25: Disturbance Rejection for Sine Reference Signal

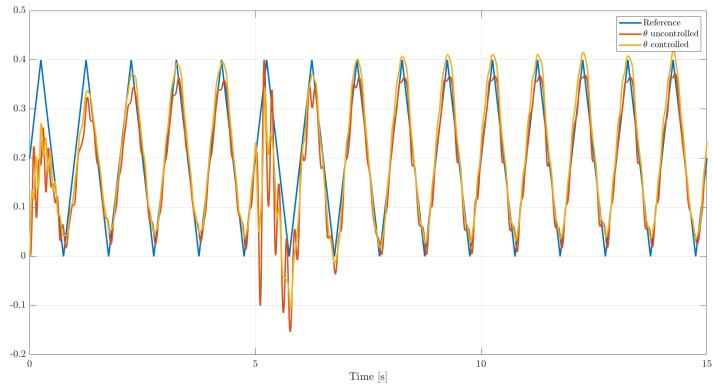


Figure 26: Disturbance Rejection for Triangle Reference Signal

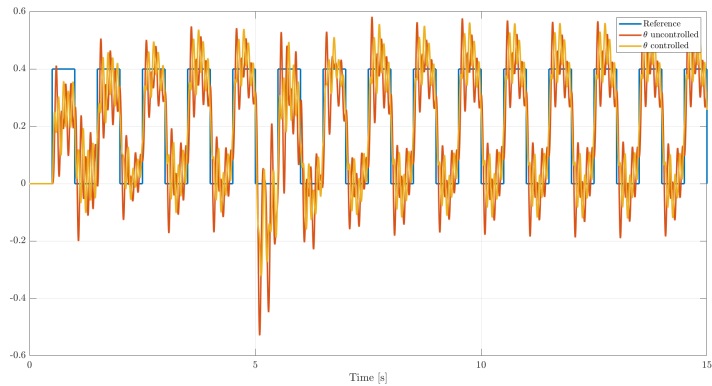


Figure 27: Disturbance Rejection for Square Reference Signal

4.3 Repetitive + Feedforward Control

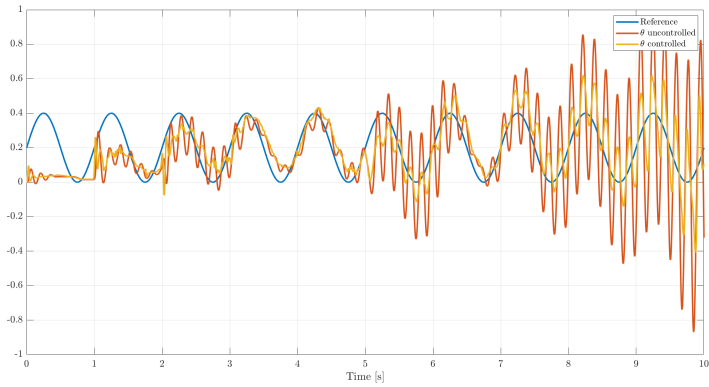


Figure 28: Disturbance Rejection for Sine Reference Signal

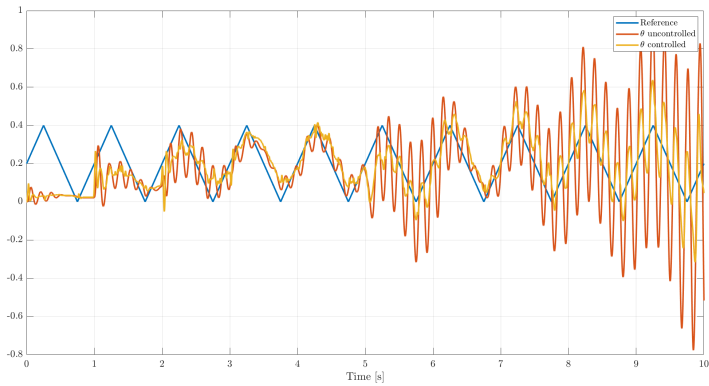


Figure 29: Disturbance Rejection for Triangle Reference Signal

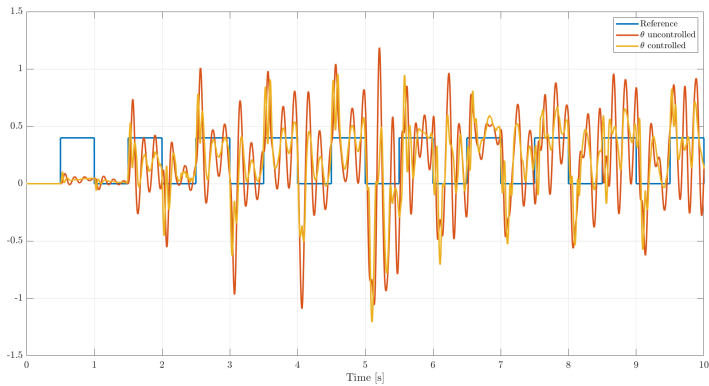


Figure 30: Disturbance Rejection for Square Reference Signal

5 Error Analysis

The tracking error for all the three controllers was analysed and found as follows:

5.1 Integral

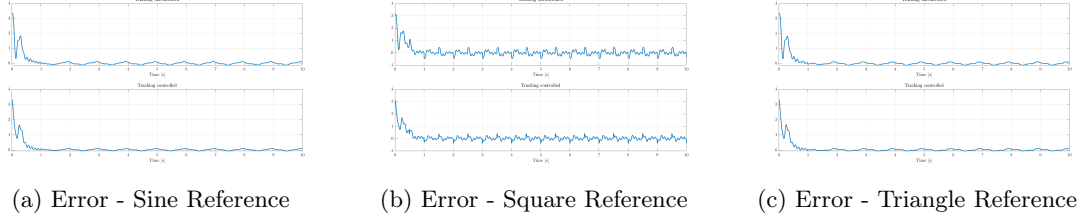


Figure 31: Tracking errors - Integral

	Controlled		Uncontrolled	
	Mean	Standard Deviation	Mean	Standard Deviation
Sine	0.0226	0.0467	-6.477×10^{-4}	0.0668
Triangle	0.0238	0.0471	-1.605×10^{-5}	0.0639
Square	0.0230	0.1335	-2.39×10^{-4}	0.1847

Table 2: Error Statistics - Integral

5.2 Integral + Oscillator

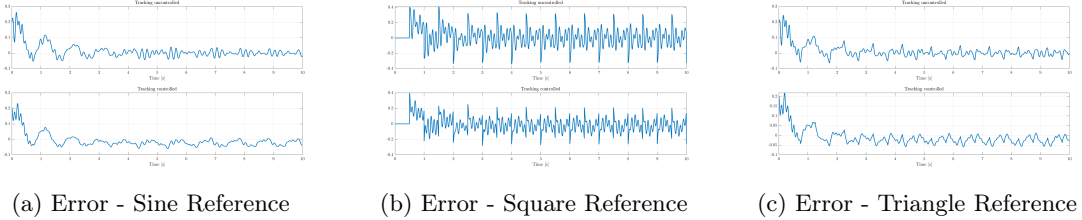
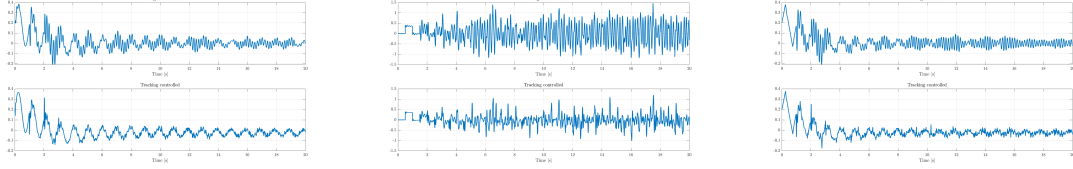


Figure 32: Tracking errors - Integral + Oscillator

	Controlled		Uncontrolled	
	Mean	Standard Deviation	Mean	Standard Deviation
Sine	-0.0227	0.016	0.0012	0.0122
Triangle	-0.0241	0.0175	-2.39×10^{-4}	0.0163
Square	-0.0239	0.0783	-3.98×10^{-4}	0.1121

Table 3: Error Statistics - Integral + Oscillator

5.3 Repetitive + Feedback



(a) Error - Sine Reference

(b) Error - Square Reference

(c) Error - Triangle Reference

Figure 33: Tracking errors - Repetitive + Feedback

	Controlled		Uncontrolled	
	Mean	Standard Deviation	Mean	Standard Deviation
Sine	-0.0234	0.0276	-3.11×10^{-4}	0.0334
Triangle	-0.0232	0.018	-8.61×10^{-4}	0.04255
Square	-0.0245	0.2836	-0.0017	0.5110

Table 4: Error Statistics - Repetitive + Feedback

We observe that the mean error in the uncontrolled motor is less than the controlled motor for all the controllers since we are observing the position of the uncontrolled motor. However, the variance in error is lesser for the controlled motor, since we are controlling the motor, resulting in a lesser deviation from the average signal.

6 Conclusions

Various system parameters of a system consisting of two motors facing each other connected by a spring are estimated. Three types of model-based controllers - integral, integral + oscillator, and repetitive + feedback controllers are implemented on the system approximated as two first-order systems connected by a spring and analysed for their performance. It is observed that the integral+oscillator controller performs better in tracking the periodic signals than the integral controller. Further tuning of gains needs to be done for the repetitive+feedback controller to get it working on the hardware.